A Modular MIMO Framework in a RAN-Level Simulator for 5G/6G Performance Evaluation: Methodology and Preliminary Results

E. Verdugo, C. Rodrigues, L. da Silva Mello and L. Lovisolo

***Abstract*— This work presents a modular Multiple-Input Multiple-Output (MIMO) framework intended to be integrated into an existing RAN-level simulator. The MIMO module follows 3GPP specifications (3GPP TR 25.996 v18.0.0 (2024-03)), supporting multiple antenna configurations and spatial channel modeling for enhanced realism. A planar array of dipole elements is implemented, and a beamforming technique is applied. A water-filling allocation strategy is used to distribute the power, and the resulting spectral efficiency is compared with the uniform power technique. The methodology is detailed, and preliminary results are presented to validate the accuracy and flexibility of the proposed framework. The existing simulator, SAMA, is a Python-based tool designed for RAN-level simulation of 5G and 6G networks. The modular approach enables realistic performance evaluation of MIMO techniques in system-level simulations, providing a valuable tool for the design and optimization of next-generation wireless networks.**

***Keywords*— 6G, MIMO, RAN simulator, water-filling.**

I. Introduction

Massive multiple-input multiple-output (MIMO) antenna arrays have moved from research prototype to baseline hardware in 5G NR macro-sites and are projected to scale into extra-large, cell-free fabrics in 6G RANs [1]. Fully exploiting the resulting degrees of freedom is very important to deliver high-speed mobile broadband (eMBB), ultra-reliable low-latency links (URLLC), and immersive extended-reality services (XR) demands. Nonetheless, the true impact surfaces only when beam management, scheduling, and inter-cell interference are analysed jointly at the system level. Most available simulators either stop at the physical link or embed rigid, MIMO implementations tied to specific software stacks, limiting exploratory studies. This paper closes that gap by introducing a modular MIMO framework inside the SAMA [2], [3] [1] RAN-level simulator, enabling plug-and-play antenna configurations and channel models for 5G/6G performance evaluation.

The literature distinguishes between link-level tools, focused on physical-layer metrics, and system-level tools that evaluate network performance. The Vienna Simulator [4] supports both scopes with modular features: 2D/3D channel models, MIMO, beamforming, Non-orthogonal multiple access (NOMA), and schedulers (best channel quality indicator - BCQI, Round-Robin), yet demands manual User Equipment (UE) and Base Station (BS) placement. Additionally, its reliance on MATLAB, a costly, closed-source platform, limits accessibility. Simu5G [5] adds end-to-end and core-network behavior but scales only to small topologies. 5G-LENA [6] and 5G-air-simulator [7] are similar tools, though with more limited scope.

For realistic service-quality analysis, a 5G RAN simulator must model UE access to physical layer resources while accounting for specific spatial RAN configurations and hardware characteristics. It must also model and simulate the radio channel variability between BS and UE to capture service heterogeneity across the area. SAMA meets these requirements: it is a system-level, CSI/CQI-driven simulator (CSI: Channel State Information; CQI: Channel Quality Indicator) [8]. Designed for multi-BS environments, SAMA incorporates beamforming-capable BSs, evaluates inter-cell interference, and implements dynamic scheduling. These features enable comprehensive RAN planning and evolution studies [2], [9].

To enable more realistic Radio Access Network (RAN) studies aligned with current technological deployments, integrating a Multiple-Input Multiple-Output (MIMO) module into SAMA is essential. As a core enabler of modern networks, MIMO enhances spectral efficiency and reliability through spatial multiplexing and diversity gains [1], [10]. Implementing MIMO modeling in SAMA will allow simulating resource allocation and performance at the system level; modeling spatial correlation, rank, and beamforming gains that shape CSI, scheduling, and inter-cell interference. This work presents the preliminary model and functionalities of a plug-in 3GPP MIMO engine, beam-steerable array models, and an SVD-based capacity calculator package to be available in the existing SAMA simulator for providing a tool for MIMO RAN benchmarking.

II. SAMA Simulator Architecture

The SAMA simulator is implemented in Python using a modular architecture, enabling flexible configuration via YAML files [11]. RAN components are modeled as classes with responsibilities aligned to their real-world counterparts. The modular design facilitates code reuse, scalability, and structural clarity, ensuring that SAMA's computational complexity scales linearly with the number of BSs and UEs. This approach allows simulations of wireless networks with large numbers of entities. The simulation workflow comprises three

Elizabeth Verdugo and L. da Silva Mello, The Department of Electrical Engineering (DEE) at the Pontifical Catholic University of Rio de Janeiro (PUC-Rio) e -mail: elizabethverdugom@gmail.com; Christian Rodrigues and Lisandro Lovisolo, Processing of Signals, Applied Intelligence and Communications Laboratory (PROSAICO), Rio de Janeiro State University (UERJ), Rio de Janeiro-RJ, e-mail: christian.rodrigues@eng.uerj.br. This work was partially supported by CNPq (processes 312743/2023-8 and 403645/2023-9) and FAPERJ.

[1] "SAMA" is the word for rope/cable in the Tupi language; it is also the acronym for Simulation and Analysis of Mobile Access.

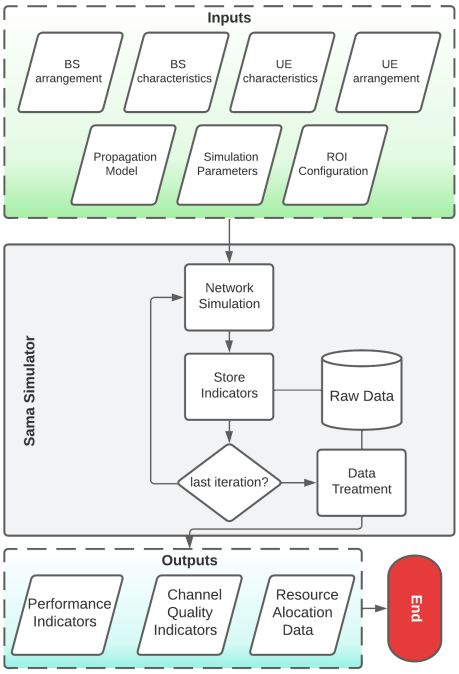

Fig. 1. The figure presents a high-level representation of SAMA's simulation process, inputs, and outputs.

stages: network setup, interference computation, and performance evaluation [2], as illustrated in Fig. 1. Following a batch of simulations, as the halting criterion, the Mann-Whitney U test is employed to assess if the probability distribution of the computed indices is statistically similar [12].

The current simulator leverages diverse configuration parameters to emulate the physical layer of mobile networks, including: definition of ROI (Region of Interest), sectored antennas with beamforming, implementation of classical schedulers from the literature (BCQI, Round Robin, and Proportional Fair-like), user positioning over the ROI via probability distributions, and BS deployment through manual configuration or clustering algorithms [2], [9]. SAMA further supports the placement of UE within the ROI via imported maps with heterogeneous user densities, alongside georeferenced building data for indoor/outdoor channel classification. This framework enables the derivation of key performance indices for mobile network evaluation while maintaining a high level of configuration and adaptation to diverse scenarios.

This work extends the reach of the evaluation provided by SAMA, embedding the MIMO channel module into it.

III. MIMO Integration in SAMA

This section describes how the new MIMO plug-in extends the grid-based system-level simulator of SAMA. We begin with design goals, then detail the antenna/array model, the geometry-based channel, the software hooks added to SAMA, and finally the capacity and resource-allocation engine.

A. Overview and Design goals

The MIMO plug-in is a self-contained module that (i) reads the BS–UE geometry (distance matrix, Angle of Departure (AoD), Angle of Arrival (AoA), device orientation), (ii) supports user-defined dipole arrays, and (iii) outputs per-link channel matrices $\mathbf{H}$ alongside high-level metrics such as RX power, rank and beam gain. This module will allow developers to use alternative channel models, hybrid/AI beamformers, or CSI-imperfect schedulers without touching the SAMA core.

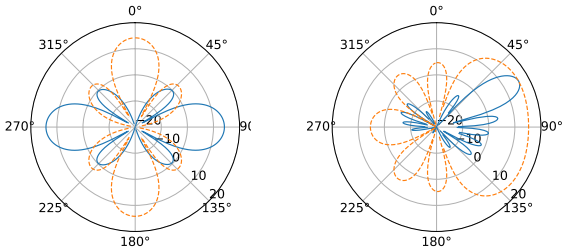

Fig. 2. Radiation patterns for two half-wavelength dipole arrays. In blue: elevation cut; in orange: azimuth cut. Left: 4x4 array, pointing toward $\theta = 90^o$ and $\phi = 0^0$, with a maximum gain of 14.19 dBi. Right: 8x4 array pointing toward $\theta = 60^o$ and $\phi = 120^o$, with a maximum gain of 16 dBi.

B. Antenna and Array Model

1) Dipole: A half-wave dipole with a far-field radiation pattern $F(\theta) = \sin\theta$ is added to the element library of SAMA. Its power pattern in spherical coordinates is $G_{\text{ele}}(\theta, \phi) = \sin^2\theta$ (azimuth-omni, 2.15 dBi).

2) Planar array and beamforming: A beamforming antenna array is synthesized by applying complex weights to each element of the array to steer the main lobe toward the desired direction (θ_0, ϕ_0) as available in the ITU-R M.2101-0 [13]. The total gain in a given direction $G_{\text{array}}(\theta, \phi)$ is computed as the sum of the responses of the individual elements weighted by the complex steering vector. It is calculated by:

$$G_{\text{array}}(\theta, \phi) = G_{\text{ele}}(\theta, \phi) + 10log[\mathbf{w}(\theta_0, \phi_0)^H \mathbf{v}(\theta, \phi)]^2 \quad (1)$$

where G_{ele} is the gain of the dipole element, $\mathbf{w}$ is the normalized beamforming weight vector, and $\mathbf{v}(\theta, \phi)$ is the array steering vector in the observation direction. Fig. 2 presents the radiation patterns for two dipole arrays developed in the simulator as an example to show.

C. Geometry-Based Channel Model

The complex-baseband signal received by a user-equipment antenna array is modeled as:

$$\bar{y} = \mathbf{H}\,\bar{x} + \bar{n} \quad (2)$$

where $\bar{y}$ is the received-signal vector (size U x 1), U being the number of antenna elements per UE and $u = 1, ..., U$ their index; $\bar{x}$ is the transmitted-signal vector (size S x 1), S being the number of antenna elements per BS and $s = 1, ..., S$ their index; $\bar{n}$ is the additive white Gaussian noise. $\mathbf{H}$ is the MIMO channel matrix (U x S) [14]. Throughout the paper, N_r denotes the total number of UEs in the scenario, and N_t the total number of BSs; these counts are distinct from the per-node antenna sizes U and S.

Following 3GPP TR 25.996 v18.0.0 (2024-03) [15], the channel is the superposition of N multipath components, each split into M sub-paths. Let:

- n = 1,..., N label the multipath components, and
- m = 1,..., M label the sub-paths inside multipath component n

The (u, s)-th entry contributed by n-th path component is:

$$h_{u,s,n}(t) = \sqrt{\frac{P_n\,\sigma_{\mathrm{SF}}}{M}} \sum_{m=1}^{M} \Bigg(\sqrt{G_{\mathrm{BS}}\big(\theta_{n,m,\mathrm{AoD}}\big)}\ \exp\Big(j\,[k d_s \sin(\theta_{n,m,\mathrm{AoD}}) + \Phi_{n,m}]\Big) \times \sqrt{G_{\mathrm{MS}}\big(\theta_{n,m,\mathrm{AoA}}\big)}\ \exp\Big(j\,k d_u \sin(\theta_{n,m,\mathrm{AoA}})\Big) \times \exp\Big(j\,k\|\mathbf{v}\|\cos\big(\theta_{n,m,\mathrm{AoA}} - \theta_v\big)\,t\Big)\Bigg). \tag{3}$$

where P_n is the power of the n-th path component; σ_{SF} is the lognormal shadow fading, applied to the n paths for a given drop (static realization of large-scale parameters, e.g., shadow fading and path angles, held constant while small-scale fading varies [15]); $\theta_{n,m,AoD}$ and $\theta_{n,m,AoA}$ are the AoD and AoA of the m-th subpath of the n-th path. $G_{BS}(\theta_{n,m,AoD})$ is the BS antenna gain, and $G_{UE}(\theta_{n,m,AoA})$ is the UE antenna gain. $k = \frac{2\pi}{\lambda}$ is the wavenumber, where λ is the carrier wavelength in meters. d_s is the distance in meters from BS antenna s from the reference ($s = 1$) antenna. d_u is the distance in meters from UE antenna u from the reference ($u = 1$) antenna. $\Phi_{n,m}$ is the phase of the m-th subpath of the n-th path. $\|\mathbf{v}\|$ and θ_v are the magnitude and angle of the UE velocity vector (not considered yet in the simulator but explained here since available in [15]).

D. Modular Framework Implementation

Several enhancements were implemented to adapt the simulator to SAMA's structure. A flexible delay model was added with three options: 3GPP, distance-based, and combined, allowing for either stochastic (i.e., lognormal) or geometry-driven delay spreads. Antenna modeling now supports dipole elements, dipole arrays, and user-defined beamforming through azimuth/elevation steering. AoD and AoA angles are computed based on BS-UE grid placement and adjusted according to sector down-tilts and antenna orientation, ensuring geometric consistency with SAMA's spatial layout.

E. Capacity and Resource Allocation

1) Capacity calculation: For every BS-UE pair, we obtain the narrow-band channel matrix $\mathbf{H}$ and decompose it with a singular-value decomposition (SVD) [14]:

$$\mathbf{H} = \mathbf{U}\mathbf{\Lambda}\mathbf{V}^{*} \tag{4}$$

where $\mathbf{U}$ and $\mathbf{V}$ are unitary rotation matrices and $\mathbf{\Lambda}$ is a diagonal matrix which collects the singular values λ_i. The higher the singular values, the larger the channel capacity. Thus, the capacity of a MIMO system is given by:

TABLE I
SIMULATION PARAMETERS

Category	Parameter	Value
Topology	Macro sites / sectors	2 sites, 3 sectors each
	UE count	500
	BS–UE distance range	62 m – 4.5 km
Carrier	Frequency (f_c)	3.5 GHz
	System bandwidth	20 MHz
BS antenna	Array architecture	2×2 dipole panel
	Element spacing	$\lambda/2$
	Peak gain (G_{BS})	8.2 dBi
	Pointing	$\phi = 90$, $\theta = 60$
	Elements per BS (S)	4
	height BS ($h_b s$)	32m
UE antenna	Elements per UE (U)	2 (omni, 0 dBi)
Channel model	Path-loss model	COST-231/Hata (suburban macro)
	Shadow fading (σ_{SF})	8 dB, log-normal
	Clusters / sub-paths	$N = 6,\ M = 10$

$$C = \sum_{i=1}^{n_{\min}} \log\left(1 + \frac{P_i\,\lambda_i^2}{N_0}\right) \text{ bits/s/Hz} \tag{5}$$

where P_i is the transmit power assigned to the i-th subchannel and N_0 is the noise-spectral density and $n_{\min} = min(N_t, N_r)$ [14].

2) Water-filling allocation method: With only a few effective eigenmodes [2] it is advantageous to apportion power unevenly across them [16]. Assuming perfect CSIT (Channel State Information at the Transmitter), we implement the classical water-filling rule, which is capacity–optimal for Gaussian MIMO links [17]. After SVD of the narrow-band channel, transmit power P_T is assigned to each eigenmode λ_i as

$$P_i = \left(\psi - \frac{N_i}{\lambda_i}\right)^{+}, \qquad \sum_i P_i = P_T, \tag{6}$$

where N_i is the noise power on mode i and ψ is the water level that satisfies the sum-power budget (cf. Eq. (12) in [17]). Stronger modes thus receive more power, weak modes possibly none; the resulting rate serves as the ideal upper bound in our benchmarks.

IV. Preliminary Results

A. Scenario description

The evaluation focuses on a suburban macro deployment whose main parameters are summarised in Table I. Two tri-sector Macro sites are located at the centre of a square region; five hundred dual-antenna UEs are dropped uniformly over the area, producing BS-UE distances from 62 m to 4.5 km. Each BS sector is equipped with a 4-panel (S=4) of 2×2 half-wave dipole array (broadside gain 8.2 dBi); UE elements are omnidirectional.

B. Propagation analysis

Path loss for every BS–UE link is computed with the modified COST-231/Hata suburban–macro expression[3] and an

[2]That is, before channel hardening effect.

[3]TR 25.996, Eq. (5.2-1) with $h_{\mathrm{bs}} = 32$ m, $h_{\mathrm{ms}} = 1.5$ m, $f_c = 3.5$ GHz and constant $C = 0$ dB for suburban macro.

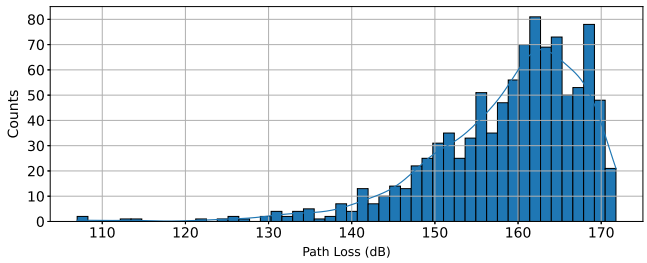

Fig. 3. Histogram of large-scale path-loss, model: COST-231/Hata suburban-macro.

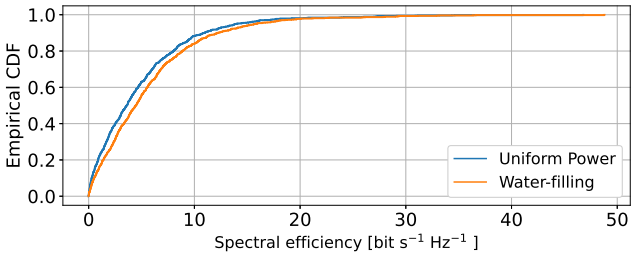

Fig. 4. Empirical CDF of per-UE spectral efficiency for the reference scenario.

8 dB log-normal shadow-fading term. Figure 3 shows the empirical distribution obtained from all 2×500 links.[4]

The calculated path losses range from 118 dB for the nearest users to 163 dB at the cell edge, with a distinct concentration between 160 dB and 170 dB. The lower tail coincides with the analytic prediction $PL_{\min} = 34.5 + 35 \log_{10} 62 \approx 118$ dB, while the upper tail is 8–10 dB below the theoretical maximum ($d = 4.5$ km), confirming that the uniform drop leaves a guard margin before the border of the region of interest.

The geometry–based engine instantiates $N = 6$ clusters with $M = 10$ sub-paths each, in accordance with TR 25.996 (§7.6). Combining the median path loss from Fig. 3 ($\approx 163\,\mathrm{dB}$), the $8.2\,\mathrm{dBi}$ sector gain and the $10 \log_{10}(NM) = 17.8\,\mathrm{dB}$ power split yields an expected per-ray magnitude of

$$20 \log_{10} |h_{u,s,n,m}| \;\approx\; -163 - 17.8 + 8.2 \;\simeq\; -172\ \mathrm{dB}.$$

A spot check over all $2 \times 500 \times 60$ rays confirms that more than 90 % of the samples lie within ± 5 dB of this value, validating the consistency between the large- and small-scale models.

C. Capacity evaluation

For every BS–UE pair, the narrow-band channel matrix $\mathbf{H} \in \mathbb{C}^{U \times S}$ is obtained as described in Section III-E.1. Singular-value decomposition $\mathbf{H} = \mathbf{U}\mathbf{\Lambda}\mathbf{V}^*$ yields the mode gains λ_i that enter the Eq. 5; power is then assigned in two ways: (i) *uniform power* (UP), $P_i = P_T / n_{\min}$; and (ii) *water-filling* (WF) as in Eq. (6).

Fig. 4 depicts the empirical CDF of the spectral efficiency achieved under both allocation techniques. WF reallocates power toward the dominant singular modes, slightly penalising the weakest links (10-th percentile: $3.7 \to 2.9$ bit s^{-1} Hz^{-1}) but expanding the upper tail: the 90-th percentile rises from 33.8 to 37.8 bit s^{-1} Hz^{-1}, ($\approx$ 12% gain). The median improves from 15.2 to 16.4 bit s^{-1} Hz^{-1} (+8%). Hence, even with a modest 2×2 array, CSI-aware water-filling delivers double-digit capacity gains for the majority of users.

V. Conclusions and Future Work

We introduced a plug-in MIMO engine for SAMA, compliant with the 3GPP clustered-channel model. The module integrates analytic dipole-array gains calculations and computes capacity via SVD, supporting both uniform and water-filling power allocation strategies. A comprehensive suburban–macro case study, including parameter table, path-loss histogram, and per-ray and link-level checks, validates the implementation and provides ready-made scripts for future scenarios.

The current release omits inter-cell interference, massive-MIMO or mmWave panels, hybrid beamforming, and data-driven beam optimization; the scheduler of the SAMA scheduler remains decoupled from the MIMO module's outputs.

Future work will focus on integrating the scheduler with MIMO outputs, modeling stochastic inter-cell interference, expanding the antenna library to support 64-T/R massive MIMO and mmWave arrays, and investigating learning-based beam management and user association strategies.

[4]Each of the two sites serves three sectors, but only the closest sector–UE pair is considered for path-loss statistics.

References

[1] J. Chen, L, Xiaohu, J. Xue, Y. Sun, H. Zhou, and X. Shen. Evolution of ran architectures toward 6g: Motivation, development, and enabling technologies. *IEEE Communications Surveys & Tutorials*, 26(3):1950–1988, 2024.

[2] C. Rodrigues. *Simulação de Redes de Acesso Rádio: Posicionamento de Estações Base e Alocação de Recursos Usando um Critério de Utilidade*. PhD thesis, Pontifícia Universidade Católica do Rio de Janeiro - PUC-Rio, Rio de Janeiro, 2023. available in: `https://doi.org/10.17771/PUCRio.acad.63113`.

[3] C. Rodrigues. Sama simulator, 2022. https://github.com/cfragoas/Sama_simulator.

[4] M Müller, F Ademaj, T Dittrich, A Fastenbauer, B Elbal, A Nabavi, L Nagel, S Schwarz, , and M. Rupp. Flexible multi-node simulation of cellular mobile communications: The vienna 5g system level simulator. *EURASIP Journal on Wireless Communications and Networking*, 2018, 2018.

[5] G Nardini, D Sabella, G Stea, P Thakkar, , and A. Virdis. Simu5G–an OMNeT++ library for end-to-end performance evaluation of 5G networks. **IEEE Access**, 8:181176–181191, 2020.

[6] N Patriciello, S Lagen, B Bojovic, , and L. Giupponi. An E2E simulator for 5G NR networks. **Simulation Modelling Practice and Theory**, 96:101933, 2019.

[7] Sergio Martiradonna, Alessandro Grassi, Giuseppe Piro, and Gennaro Boggia. 5G-air-simulator: An open-source tool modeling the 5G air interface. *Computer Networks*, 173:107151, 2020.

[8] G. Caire and S. Shamai. On the capacity of some channels with channel state information. *IEEE Transactions on Information Theory*, 45(6):2007–2019, 1999.

[9] C. Rodrigues, L. Lovisolo, and LS Mello. Alocação de recursos da interface aérea 5g a partir de um critério de utilidade. In *XL Simpósio Brasileiro de Telecomunicações e Processamento de Sinais (SBrT)*, 2022.

[10] David Tse and Pramod Viswanath. *Fundamentals of Wireless Communication*. Cambridge University Press, Cambridge, UK, 2005.

[11] Wikipedia contributors. YAML — Wikipedia, the free encyclopedia, 2022. [Online; accessed 2-October-2022].

[12] Michael P Fay and Michael A Proschan. Wilcoxon-mann-whitney or t-test? on assumptions for hypothesis tests and multiple interpretations of decision rules. *Statistics surveys*, 4:1, 2010.

[13] ITU-R P.2101-0. Modelling and simulation of IMT networks and systems for use in sharing and compatibility studies. *International Telecommunication Union, Geneva.*, 2017.

[14] David Tse and Pramod Viswanath. *Fundamentals of wireless communication*. Cambridge university press, 2005.

[15] 3GPP - Technical Specification Group Radio Access Network. Technical report 25.996 v18.0.0: Spatial channel model for multiple input multiple output (mimo) simulations). *3GPP Specification series, France.*, 2024.

[16] Marcele OK Mendonça, Paulo SR Diniz, Tadeu N Ferreira, and Lisandro Lovisolo. Antenna selection in massive mimo based on greedy algorithms. *IEEE Transactions on Wireless Communications*, 19(3):1868–1881, 2019.

[17] M. A. Khalighi, K. Raoof, and G. Jourdain. Capacity of wireless communication systems employing antenna arrays: A tutorial study. *Wireless Personal Communications*, 23(3):321–352, 2002.